Computational Materials Science 106 (2015) 170–174

Contents lists available at ScienceDirect

Computational Materials Science

journal homepage: www.elsevier.com/locate/commatsci

Phase field crystal study on the phase boundary migration induced by the Kirkendall effect ☆

Guang-Ming Lu *, Yan-Li Lu, Ting-Ting Hu, Zheng Chen

State Key Laboratory of Solidification Processing, Northwestern Polytechnical University, Xi'an 710072, China

ARTICLE INFO

Article history:
Received 30 December 2014
Received in revised form 29 April 2015
Accepted 30 April 2015
Available online 25 May 2015

Keywords:
Binary phase field crystal
Kirkendall effect
Vacancy
Phase boundary migration

ABSTRACT

The binary phase field crystal model (BPFC) was used to simulate phase boundary migration induced by the Kirkendall effect. Simulated results show that the part of the crystal located on the side with large atomic mobility experiences a shrinkage process while the part of the crystal located on the side with small atomic mobility grows outward. There are two kinds of shrinkage modes: in one, atoms melt from both sides of the phase boundary (PB) to the center one by one, in the other, only from one side of the PB to the other side. There is only one mode to grow, i.e., atoms initially nucleate in the middle of the PB and then grow toward both sides of the PB. The shrinkage and growth models were analyzed from the perspective of the free energy.

1. Introduction

Crystalline materials can satisfy working conditions after nucleation, growth, and coarsening before machining and a heat treatment process after. Interface migration may occur in every stage referred above and will determine the final grain size, which affects mechanical properties. For substitutional alloys, atoms diffuse by the vacancy-mediated mechanism when the atomic radius difference is relatively small. In the limit of the vacancy-mediated mechanism, there exists net atomic and vacancy flux in the diffusion system when the atomic mobility is unequal, which is called the Kirkendall effect [1]. Experiment has proved that diffusion processes can result in grain boundary (GB) migration [2]. However, the studies [3,4] on phase boundary migration induced by the Kirkendall effect are few. Similar simulation research on GB migration is very common. Monte Carlo method was used to simulate the GB migration in polycrystalline materials [5] and the effect of temperature on Austenite growth in C–Mn steel [6]. Molecular dynamics (MD) was used to simulate the GB migration and grain rotation mechanism [7] and the GB migration process of hexagonal close-packed metal under uniaxial stress [8], respectively. There was also a study on GB migration under uniaxial stress [9] using phase field method. Although study results above are mainly on GB migration, they can help us know more about boundary migration characteristics to some extent when we study the phase boundary migration induced by the Kirkendall effect.

The phase-field crystal (PFC) model [10,11] was derived from the density functional theory (DFT), which automatically combines many physical features, including elastic effects and crystal anisotropies due to the periodic nature of the density field. The PFC method has big advantages over traditional simulation methods (Molecular dynamics (MD), Monte Carlo, etc.), because it can simulate material behaviors on diffusional time scales and atomic length scales. It has been used to simulate many phenomena including GB migration [12–16] and Kirkendall voids [17]. In [18], the crystal motion induced by the Kirkendall effect has been studied by Elder et al. However, the vacancy and atomic diffusion paths, the diffusion behaviors of the atoms and vacancies at phase boundary were not discussed in detail in it, which is very essential to explain the phase boundary migration. The purpose of this paper is to investigate the mechanism of the phase boundary migration induced by the Kirkendall effect from the perspective of the vacancy and atom in the diffusion system we set using the binary phase field crystal (BPFC) model [19,20].

2. Simulation method

2.1. Simple binary PFC model

The PFC model is based on the traditional phase field method. A periodic function is introduced in this method allowing the representation of a periodic local time-averaged atomic density expressed in dimensionless form. Elder et al. expanded the PFC

☆ Special Issue paper Advanced Simulation Methods.

* Corresponding author. Tel.: +86 18681857801.
E-mail address: alu19620907@163.com (G.-M. Lu).

http://dx.doi.org/10.1016/j.commatsci.2015.04.047
0927-0256/

model to the form of substitutional binary alloy. The model can be written in terms of two fields, the number density difference, $n \equiv (\rho_A + \rho_B - \rho_l)/\rho_l$, and the concentration, $\psi = (\rho_A - \rho_B)/\rho_l$, where ρ_A, ρ_B and ρ_l are the atomic number densities of A atoms, B atoms and a reference liquid, respectively. In this limit, the free energy function in dimensionless form can be expressed as follows [19]:

$$F = \int d\vec{x}\left[\frac{n}{2}\Lambda^0 n - \frac{t}{3}n^3 + \frac{v}{4}n^4 + \gamma\psi + \frac{\omega}{2}\psi^4 + \frac{u}{4}\psi^4 + \frac{K}{2}|\vec{\nabla}\psi|^2\right] \quad (1)$$

where Λ^0 is the operator defined by $\Lambda^0 \equiv \Delta B_0 + B_2^l\psi^2 + B_0^x(1+\nabla^2)^2$, and $\Delta B_0 \equiv B_0^l - B_0^x$ plays the role of a normalized temperature variable. The parameter B_0^l is the dimensionless bulk modulus of the liquid, B_0^x is proportional to the elastic constants of the crystal, F is the dimensionless free energy, K is the gradient energy coefficient for the concentration field, and other parameters t, v, ω, B_2^l, u affect the phase diagram. In this paper, we select $\gamma \equiv 0$.

In this binary PFC model, the evolutions of the A and B atomic density fields is simulated using conserved dissipative dynamics of the free energy, which is expressed as follows [19]:

$$\begin{aligned}\frac{\partial n_A}{\partial t} &= M_A\nabla^2\frac{\delta F}{\delta n_A}\\ &= M_A\nabla^2[\Lambda^0 n - tn^2 + vn^3 + [w + B_2^l]\psi + u\psi^3 - K\nabla^2\psi]\end{aligned} \quad (2)$$

$$\begin{aligned}\frac{\partial n_B}{\partial t} &= M_B\nabla^2\frac{\delta F}{\delta n_B}\\ &= M_B\nabla^2[\Lambda^0 n - tn^2 + vn^3 - [w + B_2^l]\psi - u\psi^3 + K\nabla^2\psi]\end{aligned} \quad (3)$$

According to $n_A \equiv (n+\psi)/2 = \rho_A/\rho_l$ and $n_B \equiv (n-\psi)/2 = \rho_B/\rho_l$ we can get: $n = n_A + n_B$ and $\psi = n_A - n_B$. Further, the dynamical equations of motion for the density field n and concentration field ψ can be expressed below:

$$\begin{aligned}\frac{\partial n}{\partial t} &= \frac{\partial(n_A+n_B)}{\partial t} = \frac{\partial n_A}{\partial t} + \frac{\partial n_B}{\partial t}\\ &= M_A\nabla^2\frac{\delta F}{\delta n_A} + M_B\nabla^2\frac{\delta F}{\delta n_B}\\ &= (M_A+M_B)\nabla^2(\Lambda^0 n - tn^2 + vn^3)\\ &\quad + (M_A - M_B)\nabla^2\left[(w + B_2^l)\psi + u\psi^3\right]\\ &\quad + (M_B - M_A)\nabla^2 K\nabla^2\psi\end{aligned} \quad (4)$$

$$\begin{aligned}\frac{\partial \psi}{\partial t} &= \frac{\partial(n_A-n_B)}{\partial t} = \frac{\partial n_A}{\partial t} - \frac{\partial n_B}{\partial t}\\ &= M_A\nabla^2\frac{\delta F}{\delta n_A} - M_B\nabla^2\frac{\delta F}{\delta n_B}\\ &= (M_A-M_B)\nabla^2(\Lambda^0 n - tn^2 + vn^3)\\ &\quad + (M_A + M_B)\nabla^2\left[(w + B_2^l)\psi + u\psi^3\right]\\ &\quad - (M_B + M_A)\nabla^2 K\nabla^2\psi\end{aligned} \quad (5)$$

The parameters M_A and M_B are the mobilities of the A and B atoms, respectively. For simplicity, the time is non-dimensionalized such that M_A is equal to one, and the A specie is taken to be the fast diffuser ($M_A > M_B$). Simulations were conducted using a simple Euler algorithm for time derivatives and the semi-implicit Fourier spectral method [11,20,21] for Laplacian operators and higher-order Laplacian operators. Then the atomic density and concentration information can be calculated.

2.2. The determination of simulation parameters

In this simulation model, parameters that describe the liquid–solid coexistence region were used. So we choose the parameters as $B_0^l = 0.7$, $B_2^l = -1.8$, $B_0^x = 1$, $t = 0.6$, $v = 1$, $K = 4$, $w = 1$, $u = 4$. Based on the parameters chosen above, the equilibrium average value of n at liquid–solid coexistence and the equilibrium lattice constant a can be determined, i.e., $\bar{n}_{l_{eq}} = -0.2517$ in liquid, $\bar{n}_{s_{eq}} = -0.1503$ in solid and $a = 6.927$. The calculation area consists of one crystal in the central of the calculation area and the liquid region outside the solid with the size $Lx = 512\Delta x$ and $Ly = 512\Delta y$ as shown in Fig. 1. The top half of the crystal is β phase (rich in B atoms) and bottom half is α phase (rich in A atoms). The solubility of B atoms in α phase and A atoms in β phase are supposed to be large enough so that new phases are prevented from forming in the diffusion system. A periodic boundary condition is adopted in this simulation. Grid spacing and time step are $\Delta x = \Delta y = a/7$ and $\Delta t = 0.1$, respectively. The initial concentrations are $\psi = -0.1$ in β phase, $\psi = 0.1$ in α phase and $\psi = 0$ in the outmost liquid phase, respectively. The initial atomic density are $n_s(x,y,t=0) = \bar{n}_s + \frac{1}{2}(\cos(2q_y y)/2 - \cos(q_x x)\cos(q_y y)) = -0.1501 + \frac{1}{2}(\cos(2q_y y)/2 - \cos(q_x x)\cos(q_y y))$ in solid and $n_l(x,y,t=0) = \bar{n}_l = -0.2519$ in liquid, where $q_x = 2\pi/a, q_y = q_x/\sqrt{3}$. Simulations were then conducted in the area described above.

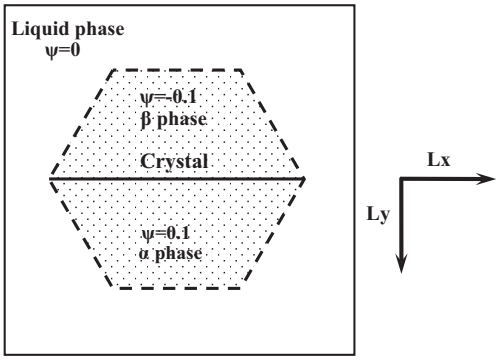

Fig. 1. The initial setup schematic of phase boundary migration induced by the Kirkendall effect.

3. Results and analysis

3.1. Phase boundary (PB) migration induced by the Kirkendall effect

To simulate the PB migration process, a crystal was set in the center of the calculation area with the initial concentration $\psi = -0.1$ (β phase, rich in B atoms) on the top side and $\psi = 0.1$ (α phase, rich in A atoms) on the bottom side, as shown in Fig. 1. The atomic mobility ratio is set to be $M_A/M_B = 100$. Fig. 2 shows the configurations of the atomic density field in the PB migration process. As can be seen in Fig. 2(b)–(f), the PBs (1, 2, 6, as indicated in Fig. 2(a)) at the top side of the crystal (rich in B atoms) migrate outward by nucleating new atomic layers. For a further study, the atoms initially nucleate in the middle of the PBs, away from corners, which then grow outward toward the corners (as indicated by the black arrows in Fig. 2(c)). The β phase at the top side grows outward layer by layer. The PBs (3, 4, 5) at the bottom side of the crystal (rich in B atoms) migrate inward by melting atoms layer by layer. There are two kinds of shrinkage modes: one is that atoms melt from both sides of the PB (4) to the center one by one, the other is only from one side of the PBs (3, 5) to the other side (as indicated by the red[1] arrows in Fig. 2(c)). Besides, the growth processes at the top side PBs appear to be faster processes than the

[1] For interpretation of color in Fig. 2, the reader is referred to the web version of this article.